Chemical Engineering and Processing 95 (2015) 347–352

Contents lists available at ScienceDirect

Chemical Engineering and Processing: Process Intensification

journal homepage: www.elsevier.com/locate/cep

Effect of type and loading of surfactant on ultrasound-assisted synthesis of $CaZn_2(PO4)_2$ nanoparticles by chemical precipitation

B.A. Bhanvase[a,*], S.H. Sonawane[b]

[a] Chemical Engineering Department, Laxminarayan Institute of Technology, RTM Nagpur University, Nagpur 440033, Maharashtra, India
[b] Department of Chemical Engineering, National Institute of Technology, Warangal 506004, Telangana State, India

ARTICLE INFO

Article history:
Received 14 March 2015
Received in revised form 5 July 2015
Accepted 14 July 2015
Available online 23 July 2015

Keywords:
Calcium zinc phosphate
Ultrasound
Surfactant type
Nucleation

ABSTRACT

In the present work, calcium zinc phosphate nanoparticles were synthesized from phosphoric acid by an ultrasound assisted precipitation method using zinc oxide (ZnO) and calcium hydroxide ($Ca(OH)_2$). The demonstration of the controlling of particle size of calcium zinc phosphate nanoparticles by the concentration of different types of the surfactants has been carried out. The application of ultrasound during the synthesis causes a supersaturation of Ca^{2+} ions in the synthesis leading to a rapid nucleation of calcium zinc phosphate nanoparticles and improves the solute transfer rate. The particle size of calcium zinc phosphate nanoparticles is significantly affected by anionic (sodium dedocyl sulfate) and cationic (CTAB) type surfactant compared to non-ionic (Span 80) surfactant. The results are well supported by employing the transmission electron microscopy (TEM), X-ray diffraction (XRD) and particle size distribution (PSD) analysis.

1. Introduction

Inorganic oxide nanoparticle pigment synthesis is growing area of research because of their excellent anticorrosive properties in coating industry. The change in properties of materials with nanometric scale in comparison with their bulk counterpart makes them increasingly suitable for a variety of applications. Some of the properties of nanomaterials such as large surface area, different crystal geometries, hydrophobicity make them more suitable for applications such as surface coatings, photocatalytic degradation, and catalytic activity and as flame retardant filler. Phosphate inhibiting pigments are considered the most feasible replacement for toxic chromates and red lead in the organic coatings of iron and steel [1–4]. Zinc phosphate is a new type of non-toxic, environmental friendly anticorrosive pigment used in coating industry with excellent anticorrosive properties. However, due to its low activity resulting from weaker solubility in electrolytes with pH 6.6–8.0, the aqueous extract of zinc phosphate weakly inhibits the corrosion of unprotected low-carbon steel and it cannot completely replace traditional toxic anticorrosive pigment [5]. As a result, to get a new generation of zinc phosphate pigments with high performance, many efforts have been made to modify zinc phosphate. To improve its activity, zinc phosphate can be modified with the addition of cation (Ca^{2+}, K^{+}, etc.) [6] or an anion (SiO_4^{4-}, MoO_4^{3-}, etc.) [7]. Dispersion of pigments having micrometer size in three-dimensional structured polymers is very difficult and also the motion of phosphate ions from the coating into the medium becomes significantly slower, which leads to an inferior anticorrosive property profile of the formed coating. This constrains need further improvement of in process for the synthesis of nanometric anticorrosive pigment.

Ultrasound is a promising technique for the synthesis of nano sized materials with narrow size particle size distribution [8–13]. Further, control of nucleation and growth rate of crystal are key factors, which decides the narrow size distribution of particles. Nucleation rate can be controlled using the addition of surfactant or using ultrasonication. Number of authors studied nucleation and growth kinetics of pigments during synthesis [14–17]. Ding and Wang [18] have prepared calcium zinc phosphate nanopowder in the presence of supersonic field by chemical precipitation using phosphoric acid, zinc oxide and calcium hydroxide as raw materials. They have studied the effect of supersonic radiation, stirring speed, reaction time and the reactant addition rate on the structure and morphologies of the new zinc phosphate media. With the aids of supersonic field, it is possible to accelerate nucleation of the media and control the growth and agglomeration of crystal nucleus effectively, which leads to the formation of spherical nanometer sized calcium zinc phosphate with uniform distribution of grain sizes. Lyczko et al. [19] have also studied the consequence of ultrasound on primary nucleation of potassium

* Corresponding author. Fax: +91 712 2561107.
E-mail address: bharatbhanvase@gmail.com (B.A. Bhanvase).

http://dx.doi.org/10.1016/j.cep.2015.07.017
0255-2701/

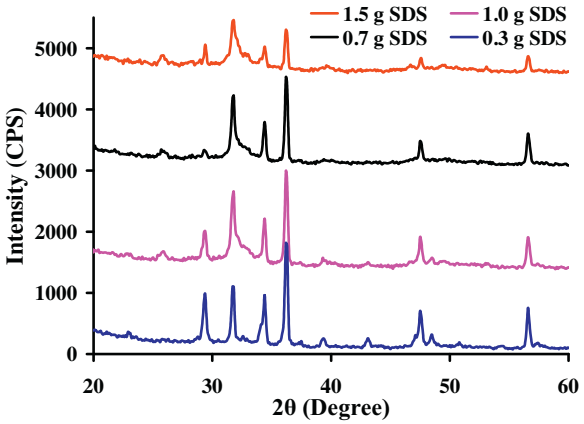

Fig. 1. Effect of SDS loading on structure of calcium zinc phosphate.

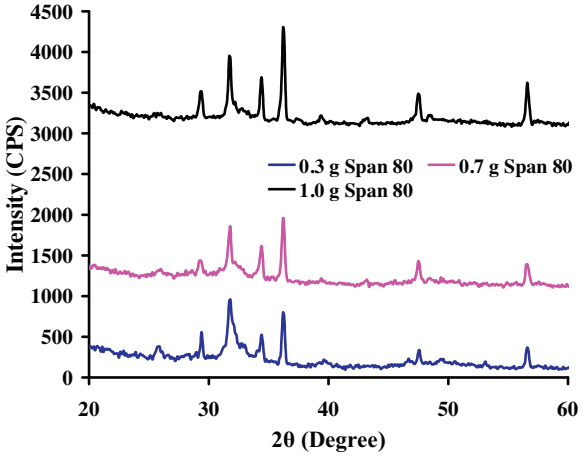

Fig. 2. Effect of Span 80 loading on structure of calcium zinc phosphate.

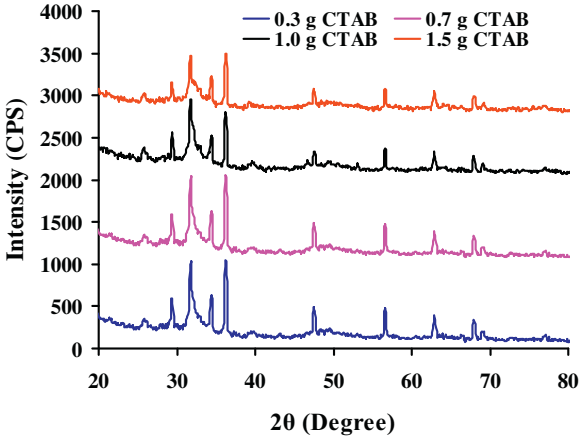

Fig. 3. Effect of CTAB loading on structure of calcium zinc phosphate.

sulfate by measuring the induction time and metastable zone width of unseeded solutions. They have reported that ultrasound reduces induction time and the metastable zone width significantly in the sonocrystallization process of potassium sulfate. By thorough literature survey, only one report was found regarding the synthesis of calcium zinc phosphate by supersonic technique.

The objective of this paper is to synthesize highly active anticorrosive calcium zinc phosphate nanoparticles by using sonochemical precipitation involving the reaction of zinc oxide and calcium hydroxide in the presence of H_3PO_4. In this work, the effect of type of surfactant, and surfactant concentration on the structure and particle size distribution of the calcium zinc phosphate nanoparticles are discussed.

2. Experimental details

2.1. Material

Analytical grade zinc oxide (ZnO), calcium hydroxide ($Ca(OH)_2$) and phosphoric acid (H_3PO_4) were purchased from S.D. Fine Chem. and used as-received without further purification. Analytical grade sodium dodecyl sulfate (SDS, $NaC_{12}H_{25}SO_4$) as a surfactant was procured from S.D. Fine Chem., Mumbai and was used without further purification. Analytical grade Sorbitan monooleate (Span 80) and Cetyl trimethylammonium bromide (CTAB) were purchased from Sigma Aldrich and used without additional purification. Millipore water was used as a medium during all the experimentation.

2.2. Preparation of $CaZn_2(PO_4)_2$ nanoparticles

The preparation of $CaZn_2(PO_4)_2$ nanoparticles was carried out according to the method reported by Bhanvase et al. [12]. To begin with, the preparation of calcium zincate media was carried out with the chemical reaction between zinc oxide (2.2 g) and calcium hydroxide (4.8 g) in 250 mL surfactant solution in the presence of ultrasonic irradiation (ultrasonic horn, frequency = 22 kHz, power = 240 W) and magnetic stirring for 20 min time. Further the dropwise addition of stoichiometric amounts of dilute H_3PO_4 was carried out to the above prepared calcium zincate media mixture in the presence of ultrasound. The reaction mass was then heated and its temperature was maintained constant at 60 °C throughout the experimentation. The addition of H_3PO_4 was accomplished within 30 min. Then the resulting reaction mixture was kept under ultrasonication for the period of 1 h. Effect of surfactant concentration of different type of surfactants such as SDS, Span-80, and CTAB on the structure and particle size distribution was studied. The white precipitate of calcium zinc phosphate material obtained was filtered and washed with water so as to remove unreacted reagents and dried in oven at 80 °C. The resultant product was characterized using XRD, TEM and particle size distribution techniques.

2.3. Characterization

The crystal structure of calcium zinc phosphate nanoparticles was recorded by using powder X-ray diffractometer (Rigaku Mini-Flox, USA) of the dried sample. The morphology of calcium zinc phosphate nanoparticles was investigated by using transmission electron microscopy (TEM), (PHILIPS,CM200, 20–200 kV, magnification 1000,000×). Particle size analysis was performed with NICOMP 380 (Particle Sizing Systems, Inc., Santa Barbara, Calif., USA) submicron particle size analyzer.

3. Results and discussions

3.1. Reaction mechanism

It has been reported that during the preparation of calcium zinc phosphate using above-mentioned process initially calcium zincate media gets formed by the reaction between calcium hydroxide and zinc oxide [18]. This calcium zincate media, then reacts with H_3PO_4 leading to the formation of calcium zinc phosphate according to the following reaction mechanism in the

Table 1
The effect of different surfactant loading on crystallographic parameters and crystallite size of the calcium zinc phosphate.

Surfactant loading	*a* (Å)	*b* (Å)	*c* (Å)	Volume (Å^3)	Crystallite size (nm)
0.3 g SDS	17.8(1)	7.42(2)	6.67(4)	847.09	34.8
0.7 g SDS	17.8(2)	7.42(2)	6.67(5)	845.71	23.4
1.0 g SDS	17.8(1)	7.41(1)	6.67(4)	844.81	23.2
1.5 g SDS	17.83(4)	7.41(1)	6.67(1)	844.50	22.9
0.3 g Span 80	17.8(2)	7.41(1)	6.67(5)	844.52	23.2
0.7 g Span 80	17.9(2)	7.41(2)	6.67(4)	848.65	23.2
1.0 g Span 80	17.85(5)	7.42(2)	6.68(3)	848.88	34.4
0.3 g CTAB	17.8(2)	7.42(2)	6.67(4)	847.64	23.2
0.7 g CTAB	17.85(7)	7.42(2)	6.67(3)	847.02	22.9
1.0 g CTAB	17.84(6)	7.42(2)	6.67(3)	846.29	22.9
1.5 g CTAB	17.8(4)	7.50(5)	6.65(2)	844.47	17.2

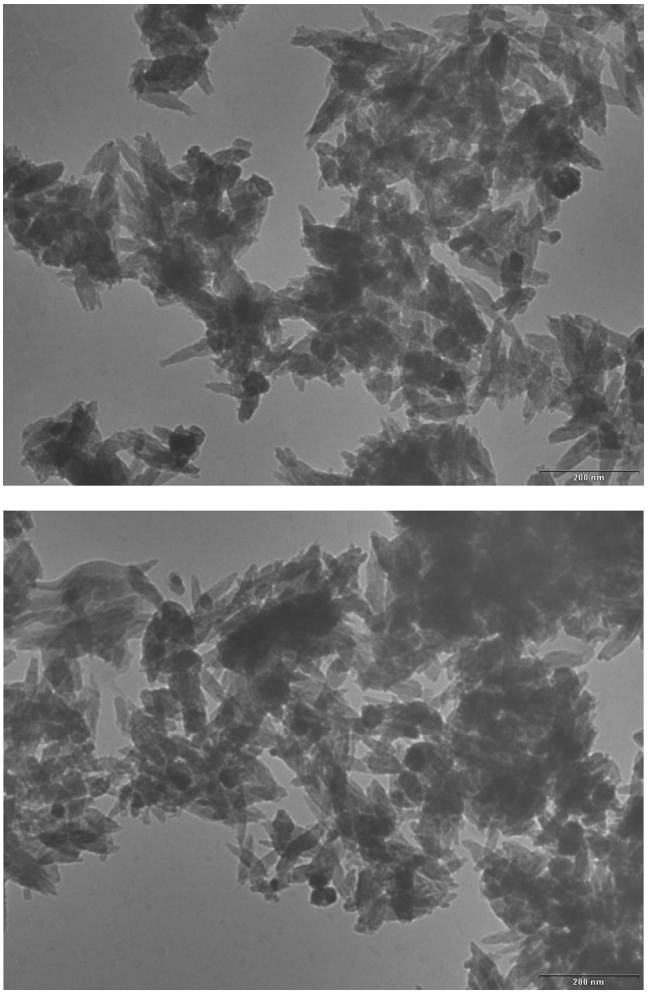

Fig. 4. TEM images of calcium zinc phosphate nanoparticles prepared with 1.5 g SDS loading in the presence of ultrasound.

presence of ultrasound.

$$Ca(OH)_2 + H_2O \rightarrow Ca^{2+}_{aq} + 2OH^- \quad (1)$$

$$OH^- + H_2O + ZnO \rightarrow Zn(OH)^-_3 \quad (2)$$

$$2Zn(OH)^-_3 + Ca^{2+}_{aq} + 2H_2O \rightarrow Ca[Zn(OH)_3]_2 \cdot 2H_2O \quad (3)$$

$$H_3PO_4 \rightarrow H^+ + PO^{3-}_4 \quad (4)$$

$$Ca[Zn(OH)_3]_2 \cdot 2H_2O + 6H^+ + 2PO^{3-}_4 \rightarrow CaZn_2(PO_4)_2 \cdot 2H_2O + 6H_2O \quad (5)$$

$$CaZn_2(PO_4)_2 \cdot 2H_2O \xrightarrow{-H_2O} CaZn_2(PO_4)_2 \cdot H_2O \xrightarrow{-H_2O} CaZn_2(PO_4)_2 \quad (6)$$

In the present work the mixture of zinc oxide and calcium hydroxide was sonicated for a 20 min. and due to strong alkalinity of calcium hydroxide, OH^- ions gets released in its aqueous suspension [20–24]. These OH^- ions can destroy the structure of ZnO in the presence of ultrasonic irradiation due to the amphoteric property of zinc oxide, leading to the formation of calcium zincate media [18]. Zinc is a reactive amphoteric metal. Further it has been reported that the generated OH^- ions forms "zincates", ZnO_2^{2-}, which are hydroxo complexes such as $Me^+[Zn(OH)_3]^-$, $Me_2^+[Zn(OH)_4]^{2-}$ and $Me_2^+[Zn(OH)_4(H_2O)_2]^{2-}$ [25] and the formed OH^- ions in the presence of ultrasound can destroy the ZnO structure.

Then the reaction between this zincate media and phosphoric acid leads to the formation of final calcium zinc phosphate product in the presence of ultrasonication.

The reaction rate gets enhanced at higher temperature. Also in an ultrasound assisted process, the nucleation rate gets increased significantly since the conditions of high temperature and high pressure generated due to cavitational effect provides energy for the nucleation and nanosized particles could be obtained. The collapse of cavities generated due to ultrasound increases the micro-mixing. This micro-mixing reduces the non-uniformity of reactant concentration in the reaction medium and accelerates the diffusion of species in the reaction medium and therefore the controlled growth of particles can be obtained. Also the powerful shock waves generated due to cavity collapse can frequently breakdown the agglomerates present in the reaction mixture and the surface adsorption of particles on each other can be avoided which results in detachment of particles in separate form and nanosized particles were obtained in this study.

3.2. X-ray diffraction analysis

The effects of different surfactants such as SDS, CTAB and Span 80 have been studied on the structure of calcium zinc phosphate nanoparticles. The X-ray diffraction patterns of ultrasonically prepared calcium zinc phosphate nanoparticles are depicted in Figs. 1–3 for various loadings of SDS, Span 80 and CTAB surfactant respectively. The X-ray diffraction patterns of the all samples have been matched with $CaZn_2(PO4)_2 \cdot 2H_2O$ in JCPDS file (Card no. 00-

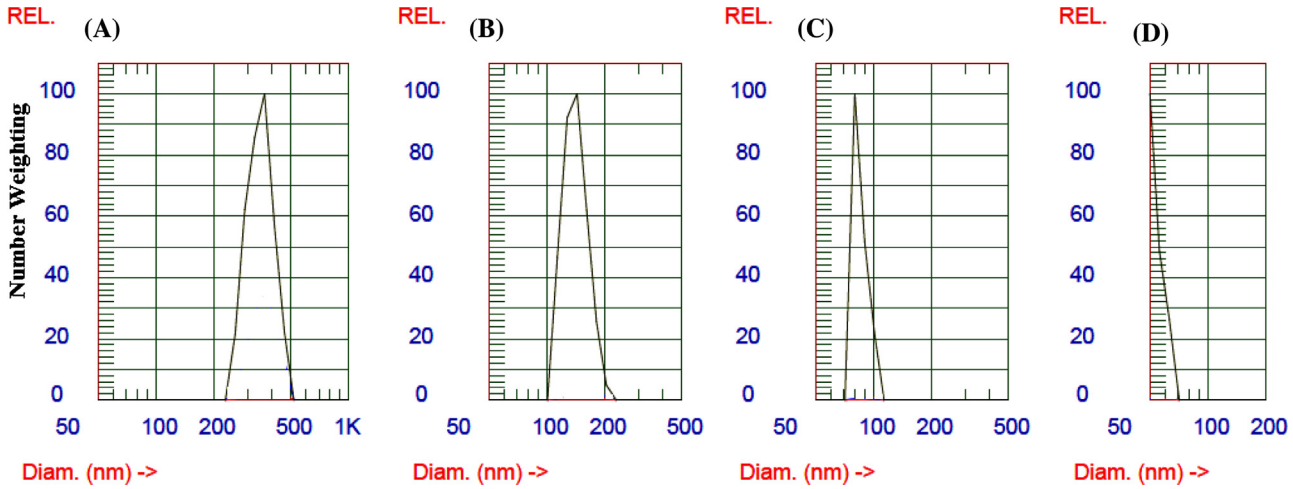

Fig. 5. Effect of SDS loading on particle size distribution of calcium zinc phosphate nanoparticles in the presence of ultrasound (A) 0.3 g, (B) 0.7 g, (C) 1.0 g and (D) 1.5 g.

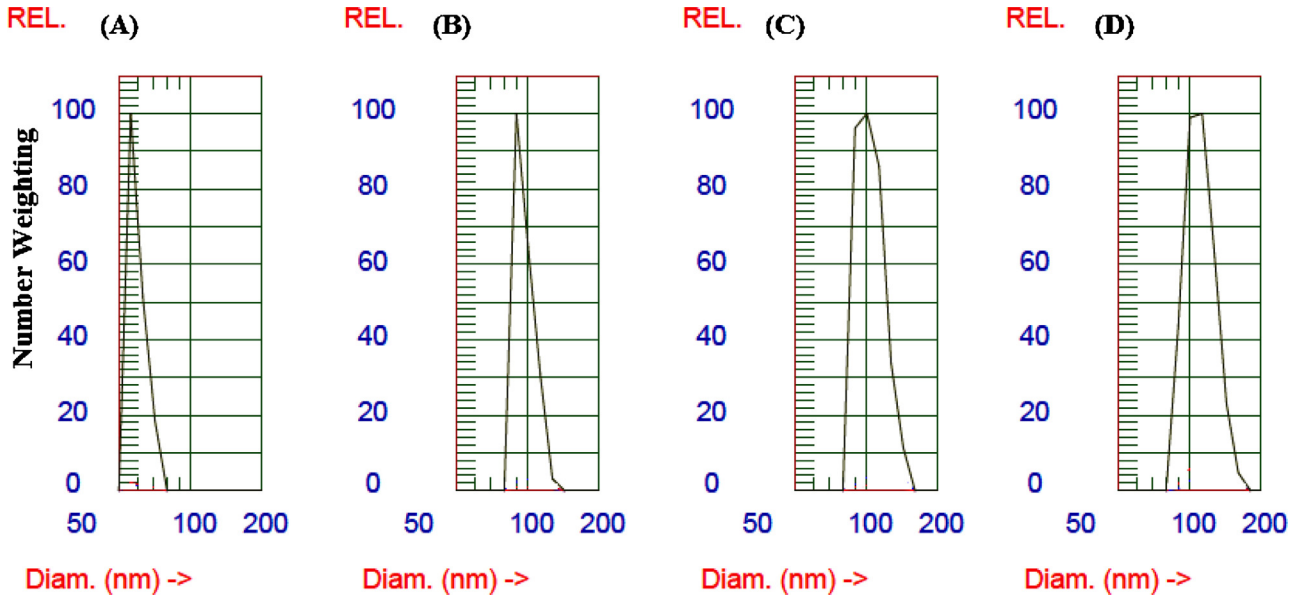

Fig. 6. Effect of SPAN 80 loading on particle size distribution of calcium zinc phosphate nanoparticles in the presence of ultrasound (A) 0.3 g, (B) 0.7 g, (C) 1.0 g and (D) 1.5 g.

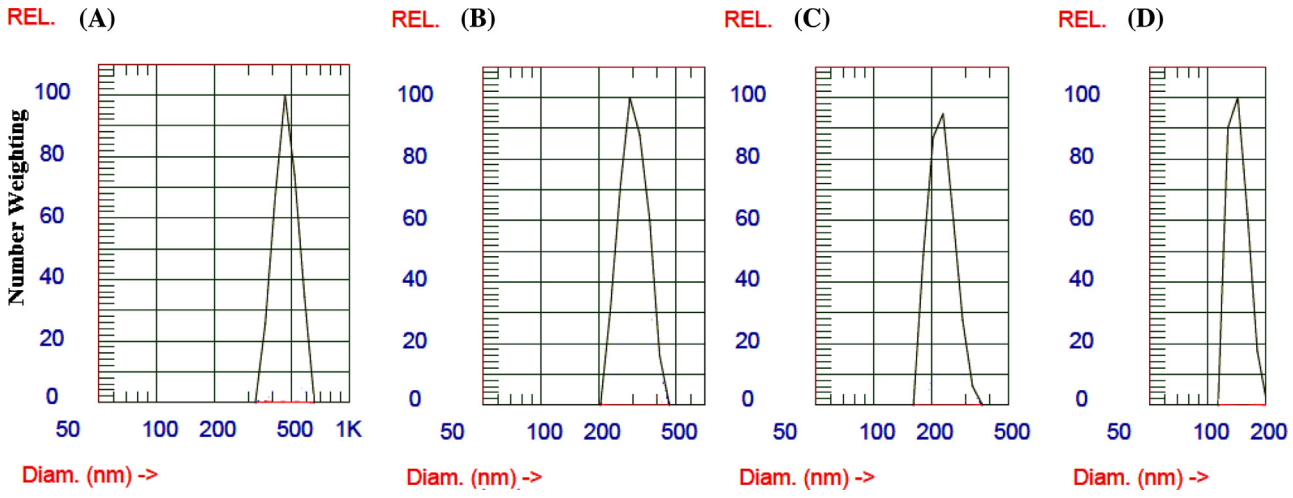

Fig. 7. Effect of CTAB loading on particle size distribution of calcium zinc phosphate nanoparticles in the presence of ultrasound (A) 0.3 g, (B) 0.7 g, (C) 1.0 g and (D) 1.5 g.

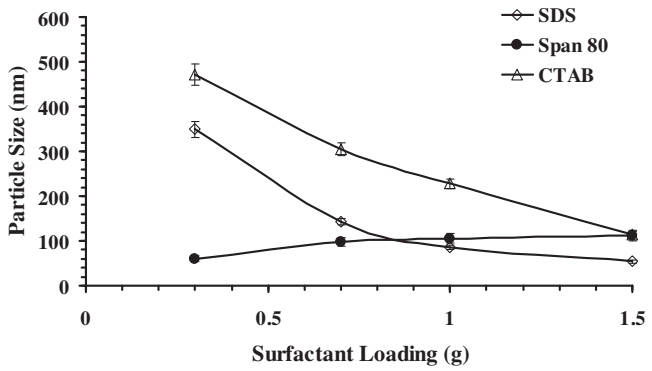

Fig. 8. Effect of surfactant on particle size of calcium zinc phosphate nanoparticles.

035-0495). The diffraction peaks at 25.9, 29.4, 31.8, 34.4, 36.4, 47.6 and 56.6° correspond to pure calcium zinc phosphate without the presence of the reactants and calcium zincate media ($Ca[Zn(OH)_3]_2{\cdot}2H_2O$). There are no peaks of impurity observed in X-ray diffraction patterns which is confirmation of the formation of pure calcium zinc phosphate nanoparticles. Further, all the peak positions in XRD patterns indicated in Figs. 1–3 are identical, indicating successful formation of calcium zinc phosphate particles. Although the peak positions are identical, the intensities of the diffraction peaks are different. In case of Fig. 1, where the effect of loading of anionic SDS surfactant on structure of calcium zinc phosphate has been studied, the peak broadening is observed with decreased intensity of peak when loading of SDS surfactant is increased. This is attributed to the change in the size of calcium zinc phosphate with SDS surfactant loading. The size of the peaks is narrower as the particle becomes bigger. Further the intensity of diffraction peaks increases with a decrease in the full width at half maximum (FWHM) of calcium zinc phosphate nanoparticles, which an indication of a possible change in the grain size. In the present study, diffraction peaks become broader with decreased peak intensity when the loading of SDS surfactant is increased from 0.3 g to 1.5 g. This indicates that calcium zinc phosphate nanoparticles are well stabilized with the increased concentration of anionic SDS surfactant by steric stabilization which inhibits coagulation of suspensions. In Fig. 2, marginal increase in the intensity of narrower peaks has been observed with an increase in the loading of non-ionic Span 80 surfactant. This indicates the increase in the particle size of the calcium zinc phosphate nanoparticles with the loading of non-ionic Span 80 surfactant from 0.3 g to 1.0 g. This is attributed to the non-ionic effect (no steric stabilization) of the Span 80 surfactant which leads to agglomeration of formed calcium zinc phosphate nanoparticles leading to the formation of larger particles. Fig. 3 depicts decrease in the intensity of broadening peaks with an increase in the loading of cationic CTAB surfactant from 0.3 g to 1.5 g. This is an indication of a decrease in the particle size with an increase in the loading of CTAB surfactant, which is attributed to stabilization of the formed calcium zinc phosphate nanoparticles by steric effect.

Further the effect of surfactant loading on the lattice constant (*a*,*b*, and *c*), volume and crystallite size estimated using Debye–Scherrer equation is depicted in Table 1. The volume and crystallite size is found to be reduced with an increase in the SDS and CTAB surfactant loading and decreased with an increase in the Span 80 loading. The possible reasons are reported above. The crystallite size is the size of one unit of calcium zinc phosphate. This is different than the particle size of the calcium zinc phosphate as particles are formed by the several units of calcium zinc phosphate molecules and gives ordered crystal shape. The observed phase of the calcium zinc phosphate from the XRD analysis is Parascholzite.

3.3. Transmission electron microscopy (TEM)

The TEM images of calcium zinc phosphate nanoparticles prepared with 1.5 g loading of SDS surfactant in the presence of ultrasonic irradiations is reported in Fig. 4. The particle size of calcium zinc phosphate nanoparticle is observed to be lesser than 50 nm. Further spindle shaped morphology of calcium zinc phosphate nanoparticle has been observed with consistent size and shape. Further, it can be seen that the morphology of the particles is homogeneous, but some nanoparticles agglomerate owing to small particle size and high surface energy. Also the observed particle size distribution is narrow with lesser agglomeration, which can be explained on the basis of the effects of ultrasonic irradiation. The particle size and shape is controlled by smaller induction period and better control of the growth rate of crystal due to ultrasonic irradiations during chemical precipitation method [10].

3.4. Effect of type and concentration of surfactant on particle size distribution

The effects of the type and the loading of the surfactant on particle size distribution of prepared calcium zinc nanoparticles in the presence of ultrasound are depicted in Figs. 5–7. Fig. 5 shows the effect of loading of SDS surfactant on particle size distribution of calcium zinc phosphate nanoparticles. The particle size range for 0.3 g loading of SDS is 230–500 nm. This size range is found to be decreased significantly with an increase in the SDS loading from 0.3 g to 1.5 g. The particle size range in case of 0.7 and 1.0 g loading is 100 to 200 nm and 70 to 120 nm. The particle size of calcium zinc phosphate nanoparticles prepared with 1.5 g SDS loading is found to be around 50 nm. Further the calcium zinc phosphate particles were formed with a fairly narrow size distribution and uniform shape could be observed. It is attributed to the significantly improved micromixing, enhanced solute transfer rate, rapid nucleation, and formation of a large number of nuclei due to the physical effects of the ultrasonic irradiation. The probable justification for this decrease in the calcium zinc phosphate nanoparticle size is also the fast kinetics of the ultrasound assisted reaction, which does not give sufficient time for the growth of particle leading to a reduction in the particle size [12]. These formed particles well stabilized with anionic SDS surfactant. However, at a low surfactant loading there is less effect on stabilization of formed nanoparticles. Hence, larger particle size is observed attributed to insufficient stabilization leading to the significant agglomeration of forming particles resulting in the formation of larger particles. With an increase in the surfactant loading formed particles were well stabilized by the SDS surfactant by steric effect and significant reduction is particle size is observed.

In case of non-ionic Span 80 surfactant such stabilization of nanoparticles by such steric effect is not observed therefore significantly larger size is observed and is found to be marginally increased with an increase in the Span 80 surfactant loading and is depicted in Fig. 6. The particle size range is observed to be 50 – 80 nm with a loading of 0.3 g surfactant. Whereas it is found to be increased to 80–130 nm, 80–170 nm and 80–185 nm when loading has increased to 0.7, 1.0 and 1.5 g respectively. Further, in case of cationic CTAB surfactant loading the particle size is found to decrease significantly and is depicted in Fig. 7. At 0.3 g loading of surfactant the calcium zinc phosphate nanoparticle size is found to be in the range of 230–650 nm and is found decreased to 200–470 nm, 170–370 nm and 110–200 nm with surfactant loading 0.7, 1.0 and 1.5 g respectively. This is again attributed to cavitation effects of ultrasound and stabilization of formed nanoparticles by steric effect.

The reduction in the average particle size with the loading of SDS, Sapn 80 and CTAB surfactant is depicted in Fig. 8. The average particle size in case of SDS surfactant is found to be decreased from 349 to 54 nm with SDS loading from 0.3 g to 1.5 g. In case of Span 80 surfactant loading from 0.3 to 1.5 g, it is found to be increased marginally from 60 to 115 nm and with an increase in the loading of CTAB from 0.3 to 1.5 g it is found to decrease from 471 to 115 nm. The possible reasons are explained as below.

The agglomeration of nanoparticles has been significantly reduced due to coating of the surfactant molecules on the particle surface and inhibits agglomeration. For the larger loading of surfactant, the surfactant allows for coating of the larger surface of nanoparticles, and this factor limits the size of the particles. At some optimum level of surfactant quantity, all the nanoparticles are coated, hence they are stabilized and the obtained particle size can be controlled. Further increase in the loading of the surfactant can only decrease the size of the nanoparticles, which finally allows for coating of all the particles. This results in the inhibition of the growth of the nanoparticles and we get lesser sized nanoparticles with an increase in the surfactant loading.

4. Conclusion

The ultrasound assisted preparation of calcium zinc phosphate nanoparticles was successfully carried out using phosphoric acid, zinc oxide (ZnO) and calcium hydroxide ($Ca(OH)_2$) precursors. It has been found that the particle size and structure of the calcium zinc phosphate is greatly affected with the loading of the different type of surfactants like SDS, Span 80 and CTAB. The use of ultrasonic irradiation during the preparation of calcium zinc phosphate causes a supersaturation of Ca^{2+} ions in the synthesis leading to a rapid nucleation of calcium zinc phosphate nanoparticles and improves the solute transfer rate. The particle size of calcium zinc phosphate nanoparticles is significantly decreased with the loading of anionic (sodium dedocyl sulfate) and cationic (CTAB) type surfactant whereas it is found to be marginally increased with the loading of non-ionic (Span 80) surfactant. The lowest average particle size is found to be 54 nm with 1.5 g loading of SDS surfactant in the presence of surfactant which is well supported by TEM images.

References

[1] N. Wheat, Protection since the lost arc. A review of primers and barrier coatings for steel, Protective Coatings Eur. 3 (1998) 24–30.
[2] J. Barraclough, J.B. Harrison, New leadless anti-corrosive pigments, J. Oil Colour Chem. Assoc. 48 (1965) 341–355.
[3] Anticorrosive Pigments, fifth ed., in: B. Elvers, S. Hawkins, G. Schulz (Eds.), Ullmann's Encyclopedia of Industrial Chemistry, vol. A201992 Chapter 4.2.
[4] R. Romagnoli, V.F. Vetere, Heterogeneous reaction between steel and zinc phosphate, Corrosion 51 (1995) 116–123.
[5] J.A. Burkill, J.E.O. Mayne, The limitations of zinc phosphate as an inhibitive pigment, J. Oil Colour Chem. Assoc. 71 (1988) 273–285.
[6] T. Nagayama, M. Yokoyama, Rust-preventive pigment composition and rust-preventive paints containing the same, US patent. US 6139616A, Oct. 31, 2000.
[7] A. Agrawal, A. Mulay, Developments in anticorrosive pigments, Paintindia 45 (1995) 49–53.
[8] B.A. Bhanvase, D.V. Pinjari, P.R. Gogate, S.H. Sonawane, A.B. Pandit, Process intensification of encapsulation of functionalized $CaCO_3$ nanoparticles using ultrasound assisted emulsion polymerization, Chem. Eng. Process 50 (2011) 1160–1168.
[9] B.A. Bhanvase, D.V. Pinjari, S.H. Sonawane, P.R. Gogate, A.B. Pandit, Analysis of semibatch emulsion polymerization: Role of ultrasound and initiator, Ultrason. Sonochem. 19 (2012) 97–103.
[10] M.A. Patel, B.A. Bhanvase, S.H. Sonawane, Production of cerium zinc molybdate nano pigment by innovative ultrasound-assisted approach, Ultrason. Sonochem. 20 (2013) 906–913.
[11] M.P. Deosarkar, S.M. Pawar, S.H. Sonawane, B.A. Bhanvase, Process intensification of uniform loading of SnO2 nanoparticles on graphene oxide nanosheets using a novel ultrasound assisted in situ chemical precipitation method, Chem. Eng. Process 70 (2013) 48–54.
[12] B.A. Bhanvase, Y. Kutbuddin, R.N. Borse, N. Selokar, D.V. Pinjari, S.H. Sonawane, A.B. Pandit, Ultrasound assisted synthesis of calcium zinc phosphate pigment and its application in nanocontainer for active anticorrosion coatings, Chem. Eng. J. 231 (2013) 345–354.
[13] M.P. Deosarkar, S.M. Pawar, B.A. Bhanvase, In-situ sonochemical synthesis of Fe_3O_4–graphene nanocomposite for lithium rechargeable batteries, Chem. Eng. Process 83 (2014) 49–55.
[14] Z. Guo, A.G. Jones, N. Li, The effect of ultrasound on the homogeneous nucleation of $BaSO_4$ during reactive crystallization, Chem. Eng. Sci. 61 (2006) 1617–1626.
[15] R.Y. Lin, J.Y. Zhang, P.X. Zhang, Nucleation and growth kinetics in synthesizing nanometer cacite, J. Cryst. Growth 245 (2002) 309–320.
[16] K. Sawada, The mechanisms of crystallization and transformation of calcium carbonates, Pure Appl. Chem. 69 (1997) 921–928.
[17] C.Y. Tai, P.C. Chen, S.M. Shih, Size-development growth and contact nucleation of calcite crystals, AIChE J. 39 (1993) 1472–1482.
[18] S. Ding, M. Wang, Studies on synthesis and mechanism of nano-CaZn2(PO4) 2 by chemical precipitation, Dyes Pigment 76 (2008) 94–96.
[19] N. Lyczko, O. Espitalier, J. Schwartzentruber, Effect of ultrasound on the induction time and the metastable zone widths of potassium sulphate, Chem. Eng. J. 86 (2002) 233–241.
[20] M. Sivakumar, A. Gedanken, Z. Zhong, L. Chen, Acoustic cavitation—an efficient energetic tool to synthesize nanosized $CuO–ZrO_2$ catalysts with a mesoporous distribution, New J. Chem. 30 (2006) 102–107.
[21] M. Sivakumar, A. Towata, K. Yasui, T. Tuziuti, T. Kozuka, Y. Iida, M.M. Maiorov, E. Blums, D. Bhattacharya, N. Sivakumar, M. Ashok, Ultrasonic cavitation induced water in vegetable oil emulsion droplets—a simple and easy technique to synthesize manganese zinc ferrite nanocrystals with improved magnetization, Ultrason. Sonochem. 19 (2012) 652–658.
[22] M. Sivakumar, A. Towata, K. Yasui, T. Tuziuti, Y. Iida, Ultrasonic cavitational activation: a simple and feasible route for the direct conversion of zinc acetate to highly monodispersed ZnO, Chem. Lett. 35 (2006) 60–61.
[23] M. Sivakumar, Sonochemical synthesis of oxides and sulfides, Theoretical and Experimental Sonochemistry Involving Inorganic Systems (2011) 191–211.
[24] M. Sivakumar, R.K. Rana, Production of nanomaterials using ultrasonic cavitation-a simple, energy efficient and technological approach, Ultrasound Technologies for Food and Bioprocessing, Springer, New York, 2011405–444.
[25] S. Budavari (Ed.), The Merck Index, Merck & Co Inc., Rahway, NJ, 1989, pp. 1597–1598.